American J. of Engineering and Applied Sciences 1 (4): 338-346, 2008
ISSN 1941-7020

Numerical Study on the Performance Characteristics of Hydrogen Fueled Port Injection Internal Combustion Engine

Rosli A. Bakar, Mohammed K. Mohammed and M.M. Rahman
Faculty of Mechanical Engineering, Automotive Excellence Center,
University Malaysia Pahang, Lebuhraya Tun Razak, 26300 Gambang,
Kuantan, Pahang, Malaysia

Abstract: This study was focused on the engine performance of single cylinder hydrogen fueled port injection internal combustion engine. GT-Power was utilized to develop the model for port injection engine. One dimensional gas dynamics was represented the flow and heat transfer in the components of the engine model. The governing equations were introduced first, followed by the performance parameters and model description. Air-fuel ratio was varied from stoichiometric limit to a lean limit and the rotational speed varied from 2500 to 4500 rpm while the injector location was considered fixed in the midway of the intake port. The effects of air fuel ratio, crank angle and engine speed are presented in this study. From the acquired results show that the air-fuel ratio and engine speed were greatly influence on the performance of hydrogen fueled engine. It was shown that decreases the Brake Mean Effective Pressure (BMEP) and brake thermal efficiency with increases of the engine speed and air-fuel ratio however the increase the Brake Specific Fuel Consumption (BSFC) with increases the speed and air-fuel ratio. The cylinder temperature increases with increases of engine speed however temperature decreases with increases of air-fuel ratio. The pressure fluctuations increased substantially with increases of speed at intake port however rise of pressure at the end of the exhaust stroke lead to reverse flow into the cylinder past exhaust valve. The fluctuation amplitude responded to the engine speed in case of exhaust pressure were given less than the intake pressure. The volumetric efficiency increased with increases of engine speed and equivalent ratio. The volumetric efficiency of the hydrogen engines with port injection is a serious problem and reduces the overall performance of the engine. This emphasized the ability of retrofitting the traditional engines with hydrogen fuel with minor modifications.

Key words: Hydrogen fueled engine, port injection, air fuel ratio, engine speed, cranks angle, performance characteristics

INTRODUCTION

In the recent days, there are two main issues regarding the fuels: availability and global climate change. The status of the availability of the fossil fuels is critical and the prices have been jumped to levels that never been reached before. Furthermore, the environmental problems are serious and the politics all over the world applied severe conditions for the automotive industry. Researchers, technologists and the automobile manufacturers are increasing their efforts in the implementation of technologies that might be replaced fossil fuels as a means of fueling existing vehicles. Hydrogen, as alternative fuel, has unique properties give it significant advantage over other types of fuel. However, the widespread implementation of hydrogen for vehicular application is still waiting several obstacles to be solved. These obstacles are standing in the production, transpiration, storage and utilization of hydrogen. The most important one is the utilization problems.

Hydrogen induction techniques play a very dominant and sensitive role in determining the performance characteristics of the hydrogen fueled internal combustion engine (H_2ICE)[1]. Hydrogen fuel delivery system can be broken down into three main types including the carbureted injection, port injection and direct injection[2].

The port injection fuel delivery system (PFI) injects hydrogen directly into the intake manifold at each intake port rather than drawing fuel in at a central point. Typically, hydrogen is injected into the manifold

Corresponding Author: M. M. Rahman, Automotive Excellence Center, Faculty of Mechanical Engineering,
University Malaysia, Pahang, Lebuhraya Tun Razak, 26300 Gambang, Kuantan, Pahang, Malaysia

after the beginning of the intake stroke. Hydrogen can be introduced in the intake manifold either by continuous or timed injection. The former method produces undesirable combustion problems, less flexible and controllable[3]. But the latter method, timed Port Fuel Injection (PFI) is a strong candidate and extensive studies indicated the ability of its adoption[3,4]. The calling sounds for adopting this technique are supported by a considerable set of advantages. It can be easily installed only with simple modification[5] and its cost is low[6]. The flow rate of hydrogen supplied can also be controlled conveniently[7]. External mixture formation by means of port fuel injection also has been demonstrated to result in higher engine efficiencies, extended lean operation, lower cyclic variation and lower NO_x production[8,9]. This is the consequence of the higher mixture homogeneity due to longer mixing times for PFI. Furthermore, external mixture formation provides a greater degree of freedom concerning storage methods. The most serious problem with PFI is the high possibility of pre-ignition and backfire, especially with rich mixtures[10-11]. However, conditions with PFI are much less severe and the probability for abnormal combustion is reduced because it imparts a better resistance to backfire. Combustion anomalies can be suppressed by accurate control of injection timing and elimination of hot spots on the surface of the combustion as suggested by[5]. Knorr *et al*.[12] have reported acceptable stoichiometric operation with a bus powered by liquid hydrogen. Their success was achieved by the following measures:

- Formation of a stratified charge by timed injection of the hydrogen into the pipes of the intake manifold with a defined pre-storage angle. At the beginning of the intake stroke a rich, non-ignitable mixture passes into the combustion chamber
- Injection of hydrogen with a relatively low temperature of 0-10°C so that the combustion chamber is cooled by the hydrogen and finally
- Lowering of the compression ratio to 8:1

One of the main conclusions drawn from the experimental study of[10] was the possibility of overcoming the problem of backfire by reducing the injection duration. Sierens and Verhelst[13] examined four different junctions of the port injection position (fuel line) against the air flow. Based on the results of their CFD model, the junction that gives the highest power output (Y-junction) was different from the junction that gives the highest efficiency (45° junction). Finally a compromise was suggested.

The present contribution introduces a model for a single cylinder, port injection H2ICE. GT-Power software code is used to build this model. The main task of this model is to investigate the performance characteristics of this engine. The emphasis is paid for the trends with the air fuel ratio and engine speed. The instantaneous behavior is also considered.

MATERIALS AND METHODS

One-dimensional basic equations: Engine performance can be studied by analyzing the mass and energy flows between individual engine components and the heat and work transfers within each component. Simulation of one-dimensional flow involves the solution of the conservation equations; mass, energy and momentum in the direction of the mean flow.

Mass conservation is defined as the rate of change in mass within a subsystem which is equal to the sum of $\dot{m}_i$ and $\dot{m}_{ee}$ from the system $\frac{dm}{dt}$:

$$\dot{m}_{sub} = \sum_i \dot{m} - \sum_e \quad (1)$$

where, subscript i and e represent the inlet and exit respectively. In one-dimensional flow, the mass flow rate ($\dot{m}$) is expressed as Eq. 2:

$$\dot{m} = \rho AU \quad (2)$$

where, ρ is the density, A is the cross-sectional flow area and U is the fluid velocity.

Energy conservation: The rate of change of energy in a subsystem is equal to the sum of the energy transfer of the system. The energy conservation can be written in the following from:

$$\frac{DE}{Dt} = \frac{DW}{Dt} + \frac{DQ}{Dt} \quad (3)$$

Where:
E = The energy
W = The work
Q = The heat

Energy conservation can be expressed as Eq. 4:

$$\overbrace{\frac{d(me)}{dt}}^{\frac{DE}{Dt}} = \overbrace{p\frac{dv}{dt} + \sum_i \dot{m}_i H + \sum_e \dot{m}_e H}^{\frac{DW}{Dt}} - \overbrace{h_g A(T_{gas} - T_{wall})}^{\frac{DQ}{Dt}} \quad (4)$$

Where:
e = The internal energy
H = The total enthalpy

h_g = The heat transfer coefficient
T_{gas} and T_{wall} = The temperatures of the gas and wall respectively

The heat transfer from the internal fluids to the pipe wall is dependent on the heat transfer coefficient, the predicted fluid temperature and the internal wall temperature. The heat transfer coefficient is calculated every time step, which is a function of fluid velocity, thermo-physical properties and the wall surface roughness. The internal wall temperature is given here as input data. Therefore, h_g can be expressed as:

$$h_g = \frac{1}{2} C_f \rho U_{eff} C_p Pr^{-\frac{2}{3}} \quad (5)$$

Where:
C_f = The friction coefficient
U_{eff} = The effective speed outside boundary layer
C_P = The specific heat
Pr = The Prandtle number

The friction coefficient is related to Renolds number which is expressed as Eq. 6:

$$R_e = \frac{\rho U_c L_c}{v} \quad (6)$$

Where:
ρ = The density
U_c = The characteristic speed
L_c = The characteristic length and v is the dynamic viscosity

The friction coefficient for smooth walls is given by:

$$C_f = \frac{16}{Re_D}, \text{where } Re_D < 2000 \quad (7)$$

$$C_f = \frac{0.08}{Re_D^{0.25}}, \text{where } Re_D > 4000 \quad (8)$$

The Prandtle number is expressed as Eq. 9:

$$Pr = \frac{\eta C_p}{\lambda} = \frac{\mu}{a} \quad (9)$$

Where:
λ = The heat conduction coefficient
μ = The kinematic viscosity and a is the thermal diffusivity

In case that the wall surface is rough and the flow is not laminar, the value of the friction coefficient then is given by Nikuradse's formula:

$$C_{f(rough)} = \frac{0.25}{(2\log_{10}(\frac{1D}{2h}) + 1.74)^2} \quad (10)$$

Where:
D = The pipe diameter
h = The roughness height

Momentum conservation: the net pressure forces and wall shear forces acting on a sub system are equal to the rate of change of momentum in the system:

$$\frac{\dot{m}}{dt} = \frac{dpA + \sum_i m_i u + \sum_i \dot{m}_e u - 4C_f \frac{\rho \dot{u} 2}{2} \frac{dxA}{D} - C_p \left(\frac{1}{2}\rho u^2\right) A}{dx} \quad (11)$$

Where:
u = Fluid velocity
D = The equivalence diameter
C_{pl} = The pressure loss coefficient
Dx = The element length. In order to obtain the correct pressure loss coefficient, an empirical correlation is used to account for pipe curvature and surface roughness, which is expressed as Eq. 12:

$$C_{pi} = \frac{p_1 - p_2}{0.5\rho u_1^2} \quad (12)$$

Where:
p_1 = The inlet pressure
p_2 = The outlet pressure
u_1 = The inlet velocity

Engine performance parameters: The brake mean effective pressure (BMEP) can be defined as the ratio of the brake work per cycle W_b to the cylinder volume displaced per cycle V_d and expressed as:

$$BMEP = \frac{W_b}{V_d} \quad (13)$$

This equation can be extended for the present four stroke engine to:

$$BMEP = \frac{2p_b}{NV_d} \quad (14)$$

Where:
P_b = The brake power
N = The rotational speed

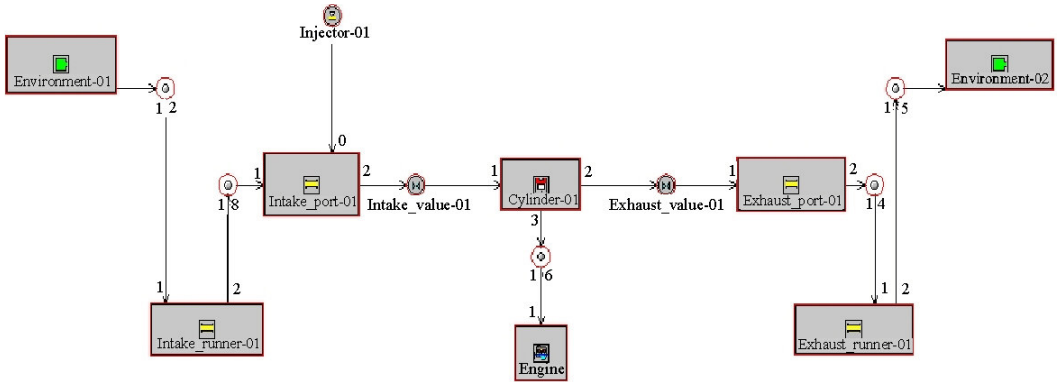

Fig. 1: Model of single cylinder, four stroke, port injection hydrogen fueled engine

Brake efficiency (ηb) can be defined as the ratio of the brake power P_b to the engine fuel energy as:

$$\eta_b = \frac{P_b}{m_f (LHV)} \quad (15)$$

Where:

$\dot{m}_f$ = The fuel mass flow rate

LHV = The lower heating value of hydrogen

The Brake Specific Fuel Consumption (BSFC) represents the fuel flow rate $\dot{m}_f$ per unit brake power output P_b and can be expressed as Eq. 16[14]:

$$BSFC = \frac{\dot{m}_f}{P_b} \quad (16)$$

The volumetric efficiency (η_v) of the engine defines the mass of air supplied through the intake valve during the intake period, $\dot{m}_a$, by comparison with a reference mass, which is that mass required to perfectly fill the swept volume under the prevailing atmospheric conditions and can be expressed as Eq. 17:

$$\eta_v = \frac{\dot{m}_a}{\rho_{ai} V_d} \quad (17)$$

where, ρ_{ai} is the inlet air density.

Engine model: A single cylinder, four stroke, port injection hydrogen fueled engine was modeled utilizing the GT-Power software. The injection of hydrogen was located in the midway of the intake port. The model of the hydrogen fueled single cylinder four stroke port inject engine is shown in Fig. 1. The specific engine parameters are used to make the model which is shown in Table 1. It is important to indicate that the intake and exhaust ports of the engine cylinder are modeled geometrically with pipes. Several considerations were made the model more realistic. Firstly, an attribute heat transfer multiplier is used to account for bends, roughness and additional surface area and turbulence caused by the valve and stem. Also, the pressure losses in these ports are included in the discharge coefficients calculated for the valves.

Table 1: Hydrogen fueled engine parameters

Engine parameter (Unit)	Measure
Bore (mm)	100.000
Stroke (mm)	100.000
Connecting rod length (mm)	220.000
Piston pin offset (mm)	1.000
Displacement (liter)	0.785
Compression ratio	9.500
Inlet valve close IVC (CA)	-96.000
Exhaust valve open EVO (CA)	125.000
Inlet valve open IVO (CA)	351.000
Exhaust valve close EVC (CA)	398.000

The in-cylinder heat transfer is calculated by a formula which closely emulates the classical Woschni correlation. Based on this correlation, the heat transfer coefficient (h_c) can be expresses as Eq. 18[15]:

$$h_c = 3.26 B^{-0.2} p^{0.8} T^{-0.55} w^{0.8} \quad (18)$$

Where:

B = The bore in meters

p = The pressure in kPa

T = Temperature in K

w = The average cylinder gas velocity in m sec^{-1}

The combustion burn rate (X_b) using Wiebe function, can be expressed as Eq. 19[16]:

$$X_b = 1 - \exp[-a\left(\frac{\theta - \theta_i}{\Delta\theta}\right)^{n+1}] \quad (19)$$

Where:
θ = The crank angle
θ_i = The start of combustion
$\Delta\theta$ = Combustion period
a and n = Adjustable parameters

RESULTS AND DISCUSSION

This search is categorized into three subsections. The first part represents the effects of BMEP, BSFC, Brake efficiency and maximum cylinder temperature with the Air-Fuel Ratio (AFR). The second part demonstrates the instantaneous results i.e. variations of intake, exhaust port and cylinder pressure against the crank angle. The third part presents the effects of engine speed (RPM) on engine performance.

It is worthy to mention that one of the most attractive combustive features for hydrogen fuel is its wide range of flammability. A lean mixture is one in which the amount of fuel is less than stoichiometric mixture. This leads to fairly easy to get an engine start. Furthermore, the combustion reaction will be more complete. Additionally, the final combustion temperature is lower reducing the amount of pollutants.

Figure 2 shows the effect of air-fuel ration on the brake mean effective pressure. The air-fuel ratio AFR was varied from stoichiometric limit (AFR = 34.33:1 based on mass where the equivalence ratio ϕ = 1) to a very lean limit (AFR =171.65 based on ϕ = 0.2) and engine speed varied from 2500-4500 rpm. BMEP is a good parameter for comparing engines with regard to design due to its independent on the engine size and speed. If torque used for engine comparison, a large engine was always seem to be better when considering the torque, however, speeds become very important when considered the power[17]. It can be seen that the decreases of the BMEP with increases of AFR and speed. It is obvious that the BMEP falls with a non-linear behavior from the richest condition where AFR is 34.33 to the leanest condition where the AFR is 171.65. The differences of BMEP are increases with the increases of speed and AFR. The differences of the BMEP are decreases 6.682 bar at speed of 4500 rpm while 6.12 bar at speed 2500 rpm for the same range of AFR. This implied that at lean operating conditions, the engine gives the maximum power (BMEP = 1.275 bar) at lower speed 2500 rpm) compared with the power (BMEP = 0.18 bar) at speed 4500 rpm. Due to dissociation at high temperatures following combustion, molecular oxygen is present in the burned gases under stoichiometric conditions. Thus some additional fuel can be added and partially burned. This increases the temperature and the number of moles of the burned gases in the cylinder. These effects increases the pressure were given increase power and mean effective pressure[15].

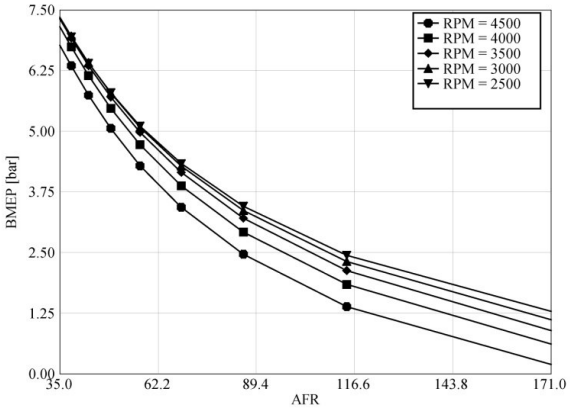

Fig. 2: Variation of brake mean effective pressure with air fuel ratio for various engine speeds

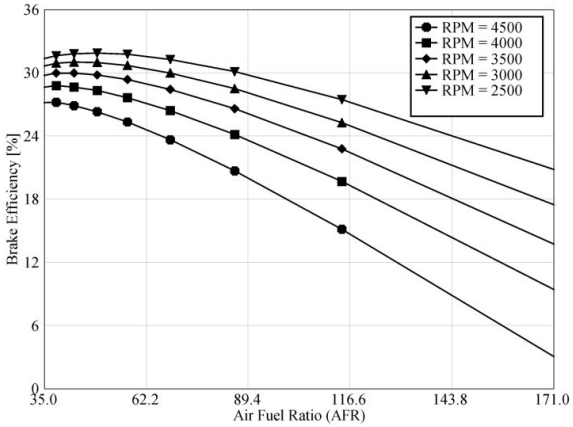

Fig. 3: Variation of brake thermal efficiency with air fuel ratio

Figure 3 shows the variation of the brake thermal efficiency with the air fuel ratio for the selected speeds. It is seen that the brake power (useful part) as a percentage from the intake fuel energy. The fuel energy are also covered the friction losses and heat losses (heat loss to surroundings, exhaust enthalpy and coolant load). Therefore lower values of ηb can be seen in the Fig. 3. It can be observed that the brake thermal efficiency is increases nearby the richest condition (AFR $\cong$ 35) and then decreases with increases of AFR and speed. The operation within a range of AFR from 49.0428-42.91250 (ϕ = 0.7-0.8) give the maximum values for ηb for all speeds. Maximum ηb of 31.8% at speed 2500 rpm can be seen compared with 26.8% at speed 4500 rpm. Unaccepted efficiency ηb of 2.88% can be seen at very lean conditions with AFR of 171.65 (ϕ = 0.2) for speed of 4500 rpm while the efficiency was observed 20.7% at the same conditions

with speed of 2500 rpm. Clearly, rotational speed has a major effect in the behavior of ηb with AFR. Higher speeds lead to higher friction losses.

Figure 4 show the behavior of the brake specific fuel consumption BSFC with AFR. The AFR for optimum fuel consumption at a given load depends on the details of chamber design (including compression ratio) and mixture preparation quality. It varies for a given chamber with the part of throttle load and speed range[15]. It is clearly seen from Fig. 4 that the higher fuel is consumed at higher speeds and AFR due to the greater friction losses that can occur at high speeds. It is easy to perceive from Fig. 4 that the increases of BSFC with decreases in the rotational speed and increases the value of AFR. However, the required minimum BSFC were occurred within a range of AFR from 38.144 (ϕ = 0.9)-49.0428 (ϕ = 0.7) for the selected range of speed. At very lean conditions, higher fuel consumption can be noticed. After AFR of 114.433 (ϕ = 0.3) the BSFC goes up rapidly, especially for high speed. At very lean conditions with AFR of 171.65 (ϕ = 0.2), a BSFC of 144.563 g kW-h^{-1} was observed for the speed of 2500 rpm while 1038.85 g kW-h^{-1} for speed of 4500 rpm. The value BSFC at speed 2500 rpm was observed around 2 times at speed 4000 rpm however around 7 times at speed 4500 rpm. This is because of very lean operation conditions can lead to unstable combustion and more lost power due to a reduction in the volumetric heating value of the air/hydrogen mixture. This behavior can be more clarified by referring to Fig. 3, where the brake efficiency reduced considerably at very lean operation conditions.

Figure 5 shows how the AFR can affect the maximum temperature inside the cylinder. In general, lower temperatures are required due to the reduction of pollutants. It is clearly demonstrated how the increase in the AFR can decrease the maximum cylinder temperature with a severe steeped curve. The effect of the engine speed on the relationship between maximum cylinder temperatures with AFR seems to be minor. At stoichiometric operating conditions (AFR = 34.33), a maximum cylinder temperature of 2752.83 K was recorded. This temperature dropped down to 1350 K at AFR of 171.65 (ϕ = 0.2). This lower temperature inhibits the formation of NO_x pollutants. In fact this feature is one of the major motivations toward hydrogen fuel.

The intake port and exhaust port pressures distributions in terms of crank angle are shown in Figure 6 and 7 respectively. The instantaneous behavior is at the 150th cycle for Wide Open Throttle (WOT)

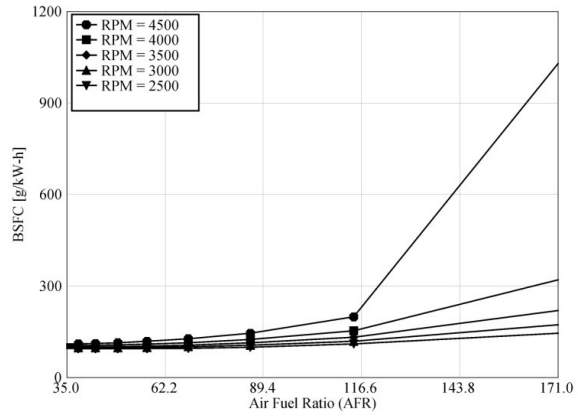

Fig. 4: Variation of brake specific fuel consumption with air fuel ratio for different engine speed

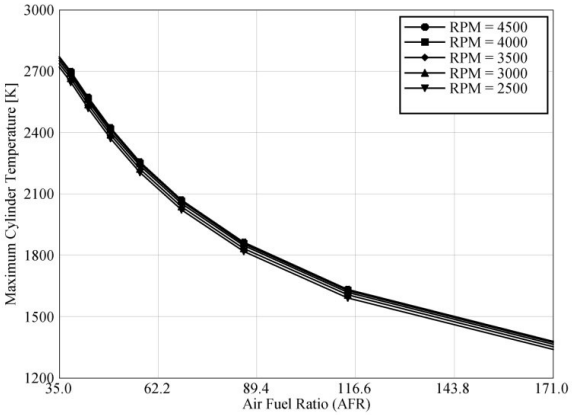

Fig. 5: Variation of maximum cylinder temperature with air fuel ratio

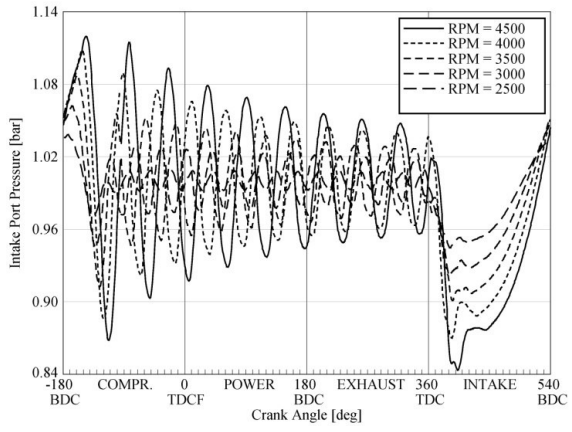

Fig. 6: Instantaneous intake port pressure distributions with crank angle for different speed

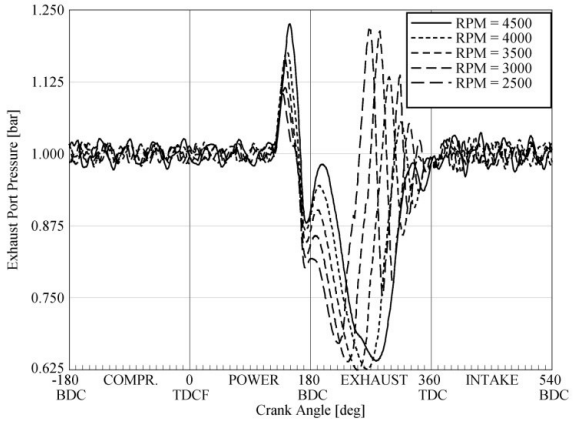

Fig. 7: Instantaneous exhaust port pressure distributions with crank angle for various engine speeds

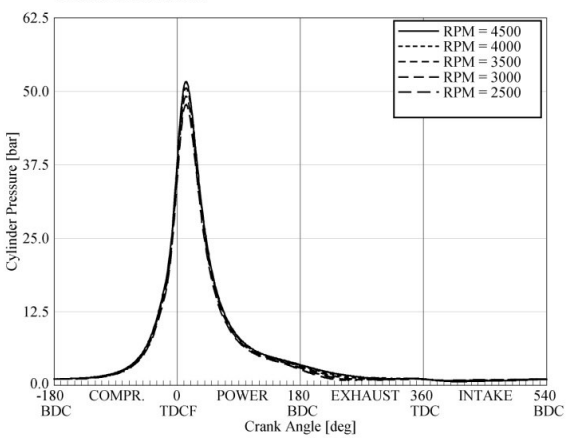

Fig. 8: Instantaneous cylinder pressure distributions with crank angle for various engine speed

and stoichiometric operation. Figure 6 and 7 are very important to investigate the backfire or pre-ignition occurrence in details. However, for the present case there is neither backfire nor pre-ignition and this is the case of normal combustion and shows typical results of pressure variation. The crank angle axis is divided into four parts to indicate the four strokes which take two cycles (720°). The pressure seems to be like a series of pulses. Each pulse is approximately sinusoidal in shape due to the single cylinder engine. The complexity of the phenomena that occur is apparent. The amplitude of the pressure fluctuations increases substantially with increasing engine speed. From Fig. 6, the maximum intake pressure was recorded 1.1144 bar at speed 4500 rpm during the compression stroke while 1.00846 bar at speed of 2500 rpm. At the suction stroke, when high intake vacuum is occurred, the curve is continuously inward and flow pulsation is small. For high speed, larger pulses can be seen. At high speeds more fuel is required and consequently more vacuum in the intake port. A vacuum of 0.8681 bar was calculated in 4500 rpm compared with 0.9897 bar at 2500 rpm. The gas dynamic effects play a very important rule here. It distorts the exhaust flow which is shown in Fig. 7. The rise of the pressure at the end of the exhaust stroke can lead to reverse flow into the cylinder past the exhaust valve, however, the high vacuum in the beginning of the first stroke is highly desired to banish the burnt gases out of the cylinder. At speed of 3000 rpm, a maximum pressure of 1.213 bar and maximum vacuum of 0.639 bar were recorded. The response of fluctuation of the amplitude to the engine speed in case of exhaust pressure seems to be less than the intake pressure.

Figure 8 shows the behavior of the cylinder pressure at the last cycle (150th cycle) for WOT and stoichiometric operation conditions. The behavior of the pressure follows the combustion phenomenon that occurs. The effect of the rotational speed on the instantaneous behavior of the cylinder pressure is minor. This curve can be divided into three parts for discussion purpose. The first part corresponds the flame development period which consumes about 5% of the air fuel mixture. Very little pressure rise is noticeable and little or no useful work is produced. The second part corresponds the flame propagation period which consumes about 90% of the mixture. During this time, pressure in the cylinder is greatly increased, providing the force to produce work in the expansion stroke. The maximum values are 51.6 bar at speed of 4500 rpm and 47.728 bar at speed of 2500 rpm. These values are less than that of traditional gasoline fuel about 70 bar with approximately similar conditions. The third part corresponds to flame termination period which consumes about the rest of the mixture (5%). In general this behavior is like the behavior of the traditional gasoline fuel, however, it is necessary to keep in mind that during the hydrogen combustion, the flame velocity is rapid and the main changes of cylinder pressure (the second part) occur in a shorter time.

Figure 9 shows the variation of the volumetric efficiency with the engine speed. In general, it is desirable to have maximum volumetric efficiency for engine. The importance of volumetric efficiency is more critical for hydrogen engines because of the hydrogen fuel displaces large amount of the incoming air due to its low density (0.0824 kg m^{-3} at 25°C and 1 atm.). This reduces the volumetric efficiency to high extent.

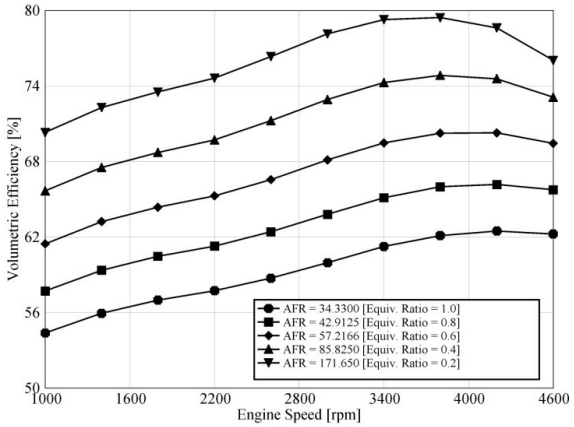

Fig. 9: Effect of volumetric efficiency with the rotational speed for different equivalence ratio

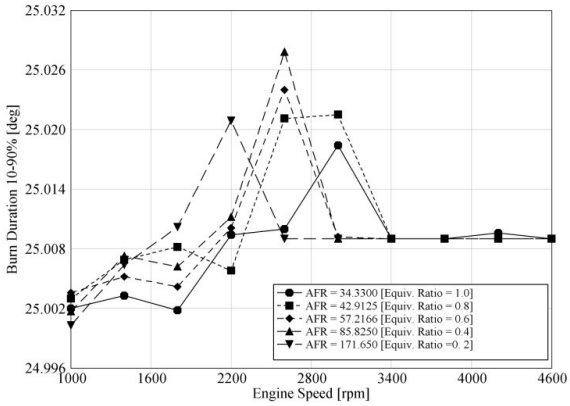

Fig. 10: Variation of combustion duration with engine speed for different equivalence ratio

For example, a stoichiometric mixture of hydrogen and air consists of approximately 30% hydrogen by volume, whereas a stoichiometric mixture of fully vaporized gasoline and air consists of approximately 2% gasoline by volume[18]. Therefore, the low volumetric efficiency for hydrogen engine is expected compared with gasoline engine works with the same operating conditions and physical dimension. This lower volumetric efficiency is apparent in Fig. 9. Leaner mixture gives the higher volumetric efficiency. The maximum volumetric efficiency was observed 79.4% at lean conditions with AFR = 171.65 (ϕ = 0.2) while 62.4% at stoichiometric conditions.

Higher speeds lead to higher volumetric efficiency because of the higher speeds give higher vacuum at the intake port and consequent larger air flow rate that goes inside the cylinder. Further increase in engine speed leads toward the maximum value of ηv For the considered speeds and with equivalence ratios of 1, 0.8 and 0.6, the maximum η_v was recorded at 4200 rpm. For equivalence ratio of 0.4 and 0.2, the maximum η_v was recorded at 3800 rpm. At further higher engine speeds beyond these values, the flow into the engine during at least part of the intake process becomes chocked. Once this occurs, further increase in speed do not increase the flow rate significantly so volumetric efficiency decreases sharply. This sharp decrease happens because of higher speed is accompanied by some phenomenon that have negative influence on η_v. These phenomenon include the charge heating in the manifold and higher friction flow losses which increase as the square of engine speed. In fact a lot of solutions were suggested to solve this problem. Furuhama and Fukuma[19] and Lynch[20] suggested and carried out tests with pressure boosting systems for hydrogen engines. White *et al*.[18] suggest direct injection (in-cylinder) for hydrogen.

Figure 10 shows the combustion duration as a function of the engine speed for different equivalence ratio. As stated earlier, hydrogen combustion velocity (1.85 m sec^{-1}) is rapid compared with that of gasoline (0.37-0.43 m sec^{-1}). Therefore short combustion duration is expected. It is well established that the duration of combustion in crank angle degrees only increases slowly with increasing speed for gasoline and diesel engines[15]. Figure 10 shows that this fact is also true for hydrogen engines. The fluctuation shown is very small, however, it was enlarged in Fig. 10 with a very high scale. All the changes take place within a range of 0.0248°. This is too small value, especially if one knows that at 4500 rpm, the crank shaft rotates 27000° within 1 sec.

CONCLUSION

The present study considered the performance characteristics of single cylinder hydrogen fueled internal combustion engine with hydrogen being injected in the intake port. The emphasis was paid to the effects of engine speed, AFR. The instantaneous behavior was also studied. The following conclusions are drawn:

- At very lean conditions with low engine speeds, acceptable BMEP can be reached, while it is unacceptable for higher speeds. Lean operation leads to small values of BMEP compared with rich conditions
- Maximum brake thermal efficiency can be reached at mixture composition in the range of (ϕ = 0.7-0.8) and it decreases dramatically at leaner conditions
- The desired minimum BSFC occurs within a mixture composition range of (ϕ = 0.7-0.9). The operation with very lean condition (ϕ<0.2) and high engine speeds (>4500) consumes unacceptable amounts of fuel
- Lean operation conditions results in lower maximum cylinder temperature. A reduction of

around 1400 K can be gained if the engine works properly at (ϕ = 0.2) instead of stoichiometric operation
- Hydrogen combustion results in moderate pressures in the cylinder. This reduces the compactness required in the construction of the engine. But, if abnormal combustion like pre-ignition or backfire happens, higher pressures may destroy the connecting rod and piston rings. Therefore, much care should be paid for this point
- The low values of volumetric efficiency seem a serious challenge for the hydrogen engine and further studied are required

In general, the behavior of the most studied parameters is similar to that of gasoline engine. This gives a great chance to retrofit gasoline engines with hydrogen fuel with minor modifications. Further future experimental work will be done to emphasize this simulation and get more details.

ACKNOWLEDGEMENT

The researchers would like to express their deep gratitude to University Malaysia Pahang (UMP) for provided the laboratory facilities and financial support.

REFERENCES

1. Suwanchotchoung, N., 2003. Performance of a spark ignition dual-fueled engine using split-injection timing. Ph.D. Thesis, Vanderbilt University, Mechanical Engineering.
2. Das, L.M., 1990. Fuel induction techniques for a hydrogen operated engine. Int. J. Hydro. Energ., 15: 833-842.. DOI: 10.1016/0360-3199(90)90020-Y
3. Das, L., R. Gulati and P. Gupta, 2000. A comparative evaluation of the performance characteristics of a spark ignition engine using hydrogen and compressed natural gas as alternative fuels. Int. J. Hydro. Energ., 25: 783-793. DOI: 10.1016/S0360-3199(99)00103-2
4. Das, L., 2002. Hydrogen engine: Research and development programs in Indian Institute of Technology (IIT), Delhi. Int. J. Hydro. Energ., 27: 953-965. DOI: 10.1016/S0360-3199(01)00178-1
5. Lee, S.J., H.S. Yi and E.S. Kim, 1995. Combustion characteristics of intake port injection type hydrogen fueled engine. Int. J. Hydro. Energ., 20: 317-322. DOI: 10.1016/0360-3199(94)00052-2
6. Li, H. and G.A. Karim, 2006. Hydrogen fueled spark-ignition engines predictive and experimental performance. J. Eng. Gas Turbines Power, ASME., 128: 230-236. DOI: 10.1115/1.2055987
7. Sierens, R. and S. Verhelst, 2001. Experimental study of a hydrogen-fueled engine. J. Eng. Gas Turbines Power, ASME, 123: 211-216. DOI: 10.1115/1.1339989
8. Yi, H.S., K. Min and E.S. Kim, 2000. The optimized mixture formation for hydrogen fuelled. Int. J. Hydro. Energ., 25: 685-690. .DOI: 10.1016/S0360-3199(99)00082-8
9. Kim, Y.Y., J.T. Lee and J.A. Caton, 2006. The development of a dual-Injection hydrogen-fueled engine with high power and high efficiency. J. Eng. Gas Turbines Power, ASME., 128: 203-212. DOI: 10.1115/1.1805551
10. Ganesh, R.H., V. Subramanian, V. Balasubramanian, J.M. Mallikarjuna, A. Ramesh and R.P. Sharma, 2008. Hydrogen fueled spark ignition engine with electronically controlled manifold injection: An experimental study. Ren. Energ., 33: 1324-1333. DOI: 10.1016/j.renene.2007.07.003
11. Kabat, D.M. and J.W. Heffel, 2002. Durability implications of neat hydrogen under sonic flow conditions on pulse-width modulated injectors. Int. J. Hydro. Energ., 27: 1093-1102. DOI: 10.1016/S0360-3199(02)00007-1
12. Knorr, H., W. Held, W. Prümm and H. Rüdiger, 1997. The man hydrogen propulsion system for city buses. Int. J. Hydro. Energ., 23: 201-208. DOI: 10.1016/S0360-3199(97)00045-1
13. Sierens, R. and S. Verhelst, 2003. Influence of the injection parameters on the efficiency and power output of a hydrogen fueled engine. J. Eng. Gas Turbines Power, ASME., 125: 444-449. DOI: 10.1115/1.1496777
14. Blair, G.P., 1999. Design and Simulation of four Stroke Engines. 1st Edn., SAE International Society of Automotive Engineers Inc., Warrandale, Pa., USA., ISBN: 978-0-7680-0440-3, pp: 840.
15. Heywood, J.B., 1988. Internal Combustion Engine Fundamentals. 1st Edn., McGraw-Hill, London, ISBN-10: 007028637X, pp: 930.
16. Ferguson, C.R. and A.T. Kirkpatrick, 2001. International Combustion Engines: Applied Thermosciences. 2nd Edn., John Wiley and Sons, Inc., New York, ISBN: 10: 0471356174, pp: 384.
17. Pulkrabek, W.W., 2003. Engineering Fundamentals of the Internal Combustion Engines. 2nd Edn., Prentic Hall, New York, USA., ISBN: 10: 0131405705.
18. White, C.M., R.R. Steeper and A.E. Lutz, 2006. The hydrogen-fueled internal combustion engine: A technical review. Int. J. Hydro. Energ., 31: 1292-1305. .DOI: 10.1016/j.ijhydene. 2005.12.001
19. Furuhama, S. and T. Fukuma, 1986. High output power hydrogen engine with high pressure fuel injection, hot surface ignition and turbocharging. Int. J. Hydro. Energ., 11: 399-407. .DOI: 10.1016/0360-3199(86)90029-7
20. Lynch, F.E., 1983. Parallel induction: A simple fuel control method for hydrogen engines. Int. J. Hydro. Energ., 8: 721-730. DOI:10.1016/0360-3199(83)90182-9